Three-dimensional Vortical Structures in the Wake of a Flexible Flapping Foil

by

Matthew J. Krueger

Submitted to the Department of Mechanical Engineering in Partial Fulfillment of the Requirements for the Degree of

Bachelor of Science

at the

Massachusetts Institute of Technology
June 2005

MASSACHUSETTS INSTITUTE OF TECHNOLOGY
JUN 08 2005
LIBRARIES

© 2005 Matthew J. Krueger
All rights reserved

The author hereby grants to MIT permission to reproduce and to distribute publicly paper and electronic copies of this thesis document in whole or in part.

Signature of Author.....
Department of Mechanical Engineering
March 7, 2005

Certified by.....
Alexandra H. Techet
Assistant Professor of Mechanical and Ocean Engineering
Thesis Supervisor

Accepted by.....
Ernest G. Cravalho
Professor of Mechanical Engineering
Chairman, Undergraduate Thesis Committee

ARCHIVES

Three-dimensional Vortical Structures in the Wake of a Flexible Flapping Foil

by

Matthew J. Krueger

Submitted to the Department of Mechanical Engineering
On May 6, 2005 in Partial Fulfillment of the
Requirements for the Degree of Bachelor of Science in
Mechanical Engineering

ABSTRACT

This project aims to gain a qualitative view of the three-dimensional vortical structures of a flexible flapping foil at Reynolds number 164. Flexible foils were fabricated, coated with fluorescent dye, and towed with heave and pitch in a large glass tank. The foil cross section is a NACA 0030 foil shape, and the foil has an aspect ratio of 3. Pictures where taken of the vortical structures from planform, wingtip, and isometric views over a range of Strouhal number and kinematic parameters. Results are compared to previous experimental and numerical studies.

Thesis Supervisor: Alexandra H. Techet
Title: Assistant Professor of Mechanical and Ocean Engineering

Acknowledgements

I would like to thank my thesis advisor Alex Techet, for making this thesis such a joy to work on. Also Melissa Read, whose patience and willingness to help was much appreciated. Thank you Mom and Dad, your constant support has always guided me. All my friends and family, who have made my life so fun and amazing. And Jaclyn, thank you for always believing in me and bringing me up when I'm down. Thank you all from the bottom of my heart.

Table of Contents

Chapter 1

Introduction

Fish are known to be excellent swimmers. Their ability to swim and maneuver effectively has evolved over centuries. Typically fish swim by undulating their bodies and flapping their tails. This motion generates thrust that propels the fish forward. Many studies of fish swimming hydrodynamics have looked at flapping foils as a model for the fish tail. Studies have been widely restricted to two-dimensional flow visualization and force measurements. The three-dimensional nature of a thrust wake produced by flapping foils and swimming fish is not widely understood. This thesis aims to gain a qualitative view of the three-dimensional shape of vortical structures in the propulsive wake of a heaving and pitching (i.e. flapping) hydrofoil.

Typically a reverse von Kármán vortex street is seen in thrust generating wakes, as opposed to the famous von Kármán street created by drag producing wakes. The reverse von Kármán street produces a net thrust as each vortex spins in the opposite direction than those that produce drag forces. In Figure 1 below from Freymouth (1988) a von Kármán street (top) and reverse street (bottom) are shown generated by an airfoil.

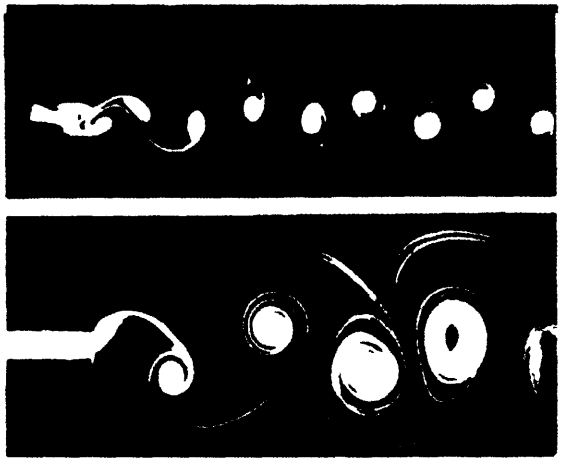

Fig. 1 Top: vortex street shed from a circular cylinder at $Re = 120$ (cylinder diameters 0.63 cm, flow speed $U_o = 30.5$ cm/s). Bottom: vortex street generated behind the trailing edge of an airfoil pitching periodically around the quarter-chord axis (chord length $c = 35.6$ cm.
From Freymouth(1998).

Two recent publications of note have produced images of the three-dimensional vortical structures in flapping foil wakes. In von Ellenrieder et al. (2003) a NACA0030 foil oscillated in heave and pitch in a circulating water tunnel. Dye was injected through small ports in the foil, which left streaklines representing the vortical structures that were then photographed from the side and top. Secondly, Guglielmini (2004) simulated the flow past a similar flapping foil and looked at the wake patterns. Both experiments were performed with the same foil and kinematic heave and pitch parameters; however, strikingly different vortical structures were found in each study. The purpose of this thesis is to confirm or contest both studies.

Like von Ellenrieder et al. (2003), we used dye to view the streaklines created in the wake, but instead of a re-circulating water tunnel, a 30 gallon glass tank was used as a tow tank. Towing the foil through a quiescent tank will yield clean results unaffected by flow velocity fluctuations often found in circulating water tunnel. Even a small current can distort the streaklines coming off of the foil, making the tank a better choice for viewing the flow patterns. Data obtained in this study will be closely compared with the von Ellenrieder and Guglielmini results in chapter 3.5.

Chapter 2

Experimental Setup

2.1 The Flapping Foil

In this study a flexible foil made from Dow Corning HS III latex rubber was used, in order to more closely represent the flexibility of a fish tail. This is a departure from the aluminum used in the previous studies and those done by von Ellenrieder; however, Melissa Read will soon be performing her thesis with a rigid foil. Dow Corning HS III was chosen due to its high strength and flexibility. The foils were made using an aluminum mold for a NACA 0030 foil. The NACA 0030 foil is a symmetric foilshape with a chord length of c=19 mm, maximum thickness t, where t/c=0.3, and aspect ratio AR=3.0. The foil was molded to an 1/8'' steel rod at the quarter-chord point.

A sample of the HS III was made and tested on a Bose/EnduraTEC Elf 3200 to determine the Young's Modulus. The HS III had significant visco-elastic properties, as the modulus increases with frequency when viscose properties do not have time to develop. At our experimental frequencies (from 0.1 to 1 Hz) a Young's Modulus of 181 kPa was found. Although extremely flexible, the material was not seen to flex significantly in our tests.

Fluorescent dye was applied to the foils by first mixing the dye with Elmer's glue to help the dye adhere to the foil. Because the glue is water-soluble the dye came off easily in water. The dye-glue mixture was applied to the foil at least a half-hour before the foil was used so the glue could dry and stick to the foil. The glue was applied with a thin mixing stick. Care was taken to continually coat the mixture evenly over the foil because the mixture has a tendency to clump up leaving uncoated portions. A dried and ready foil is shown in Figure 2.

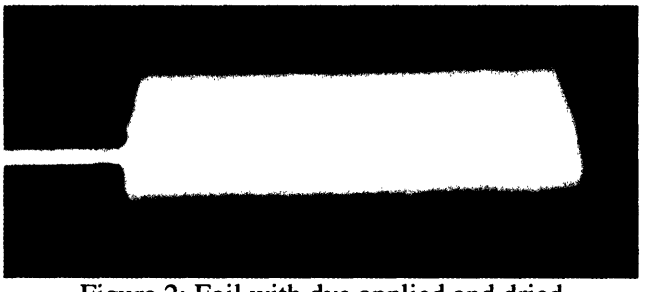

Figure 2: Foil with dye applied and dried

2.2 The Apparatus

The test apparatus shown schematically in Figure 3 towed the foil along the lead screw while the carriage oscillated in heave and pitch. The lead screw is activated by a motor which is programmable through a control box. The lead screw's control box needed to be programmed only once, as each run was towed at the same speed. A stepper motor on the carriage was controlled by a separate control box. The speed of the stepper motor set the frequency with which the foil heaved and pitched, which is always equal. To create heave motion, the two shafts were simply misaligned to create sinusoidal travel. A linkage from this shaft to the foil's shaft created pitch. By changing alignment settings on the carriage the maximum pitch amplitude and phase angle between heave and pitch could be varied. Two linear bearings on the carriage allowed the foil to smoothly heave and pitch.

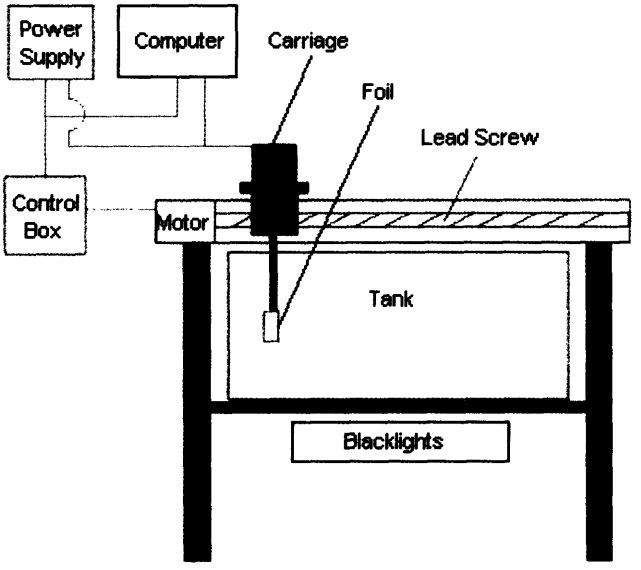

Figure 3: Schematic diagram of test apparatus

To illuminate the flow patterns, two 15 W fluorescent light bulbs were placed below and to the side of the tank. A Sony Cyber-shot 5.0 mega pixel camera was used to photograph the wake. Because only one camera was available, planform (side) and wingtip (bottom) views were recorded subsequently. Also, because of the long travel, the foil was followed and photographed by hand. Isometric views were recorded from an angle above and behind the foil, through the free surface. Thus, some distortion is evident in the isometric views as the free surface was not completely flat.

2.3 Experimental Procedure

The equation of motion for heave and pitch are defined respectively as

$$h(t) = h_0 \cos(2\pi f t) \qquad \text{(Eq. 1)}$$

and

$$\theta(t) = \theta_o \cos(2\pi f t + \varphi), \qquad \text{(Eq. 2)}$$

where h_0 is heave amplitude, θ_0 is pitch amplitude, f is oscillation frequency, and φ the phase angle between heave and pitch. The relationship between heave and pitch is shown in Figure 4. The heave amplitude is held constant at $h_0 = c/2$, while the pitch amplitude θ_0, frequency f, and phase φ are varied as test parameters. The Strouhal number, $St = 2h_0 f / U$, where U is the forward speed of the foil, is varied depending on the frequency f. Three independent tests are preformed testing the effects of Strouhal number, pitch amplitude, and phase angle between heave and pitch. All tests were performed at Reynolds number 164 based on foil chordlength. Each test is summarized in table 1.

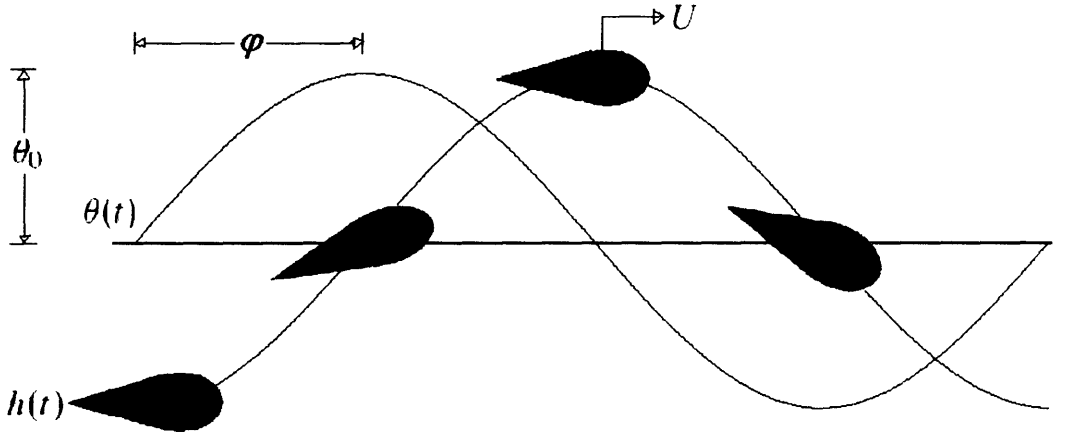

Figure 4: Heave and pitch profiles for $\varphi = 90°$

Table 1: Test parameters for flow visualization

Test	St	θ_0 (deg)	φ (deg)
1	{0.2, 0.25, 0.3, 0.35, 0.4}	10	90
2	0.35	{0, 5, 10, 15, 20}	90
3	0.35	10	{60, 75, 90, 105, 120}

After every run the tank was emptied with a bilge pump, and then refilled with fresh water. While emptying and filling the tank, the used foil was repainted, the carriage was removed and fitted with a new foil, and the parameters were set. The mold was used to align the foil on the centerline of heave at zero pitch angle, while pins were used to align the maximum pitch amplitude θ_0 and phase angle, φ. Once filled, the tank was allowed to settle for a minimum of five minutes. Last, the room lights were turned off, the carriage was lowered into position and secured, and the towing and carriage motors were activated. Care was taken to not bump the tank while fastening the carriage and taking pictures in order to maintain a still water column.

Chapter 3

Results and Discussion

3.1 Overall Flow Structure

The fluorescent dye created very vivid flow shapes seen in Figure 5 below. See Appendix A for images from every parameter set. All pictures are shown with the foil traveling from right to left. In the wingtip view, the vortices are easily seen spinning back towards the foil and creating net thrust, as seen in the airfoil in Figure 1. The vortices form rings easily seen in the planform views. The rings were seen in every parameter set and seem to be a product of three-dimensional edge effects. Considering an infinitely long foil, these rings would not be seen from the planform angle. However, the vorticity pattern seen from the wingtip would still be seen.

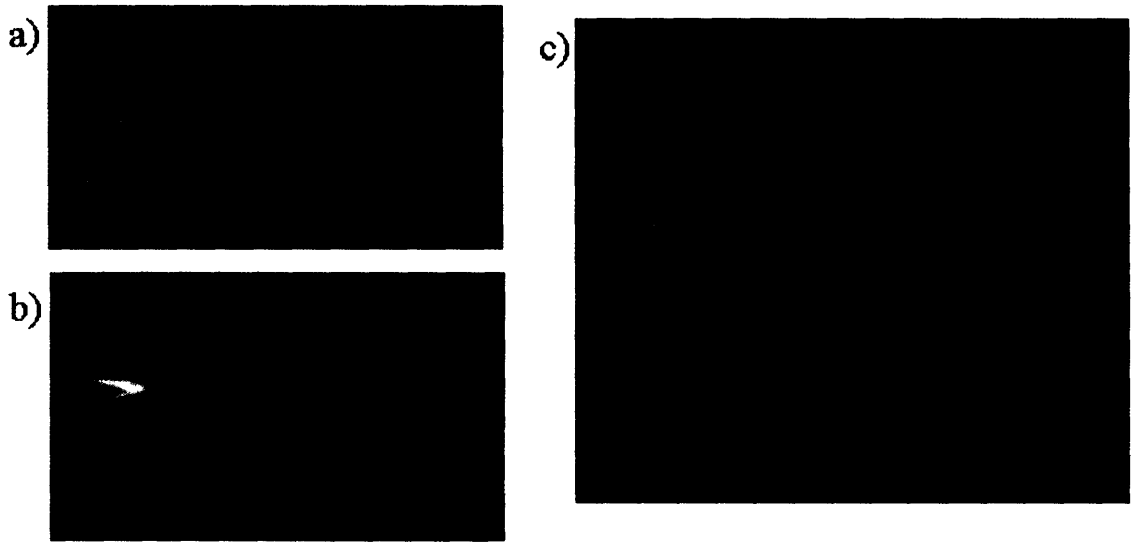

Figure 5: Pictures from parameters St=0.35 θ_0=5° φ=90°; a) Planform view, b)Wingtip view, c)Isometric view

The images were not taken simultaneously, and so are best for gaining an overall understanding of the flow shapes. However, inferences about the timing of the vorticity patterns can still be made from the wingtip view. Notice in Figure 5 b) that the foil is

approximately at its maximum heave position. At this position, the vortex from its minimum heave is no longer touching the foil as the beginnings of the next vortex begins to roll off of the trailing edge. This vortex formation and release timing was seen throughout the study. The vortices form as they curl towards the lower pressure side of the foil. This lower pressure is formed as the foil pushes water out of the way and sucks in water behind it. Examining Figure 5 b) closely, one can see a vortex forming as fluid rushes to the low pressure side from the top over the trailing edge, from the bottom of the leading edge, and from the top and bottom planform edges. The flow to this low-pressure zone creates the vortex ring seen in the isometric view.

3.2 Strouhal Number Effects

As the Strouhal number increases so does the number and relative strength of vortices. Figure 6 shows the wingtip view of each of the five cases. Because the Reynolds number was set constant for all cases considering only forward movement, these results are slightly misleading. For the case of St=0.4, the foil traveled twice as many cycles in the same distance as when St=0.2. This increase of cycles also represents an increase of velocity and Reynolds number. Accordingly more cycles are seen for higher Strouhal numbers. Also, the higher Strouhal numbers produce more pronounced vortices which curl around more than 180°. The lower Strouhal numbers do not show as much vorticity as they keep more of the sinusoidal shape of the foil's travel. The vortices which curl the most create a stronger forward net force, increasing thrust; thus, the higher Strouhal numbers lead to more thrust.

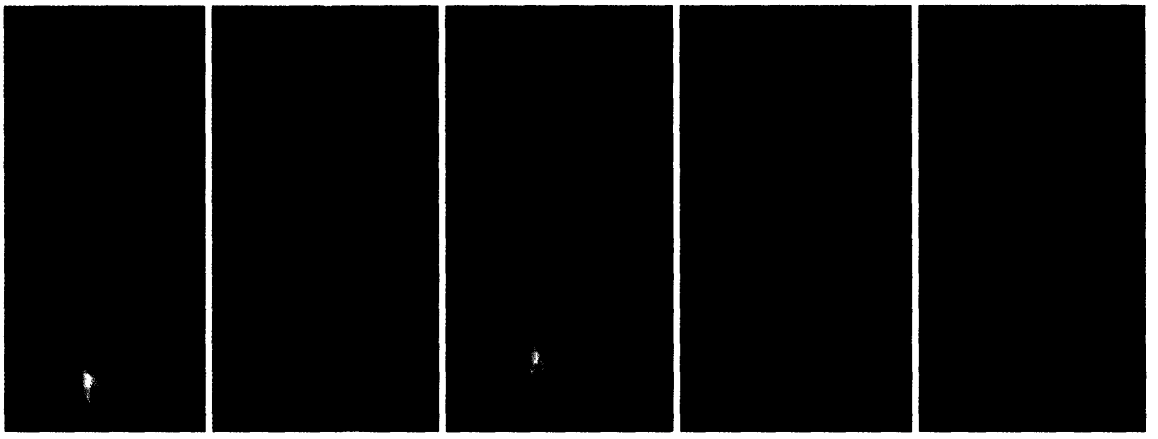

Figure 6: Wingtip views for increasing Strouhal numbers, θ_0=10° φ=90°;
a) St=0.2, b) St=0.25, c) St=0.3, d) St=0.35, e) St=0.4

3.3 Pitch Amplitude Effects

For increasing pitch amplitude, the foil rotated faster, and thus, larger forces were exerted. These larger forces seem to have made stronger vorticity, as noticeable in Figure 7 e) where the vortex curves more than 180°. Also, the zero pitch case is interesting in that no pitching is necessary to still form a vortex pattern.

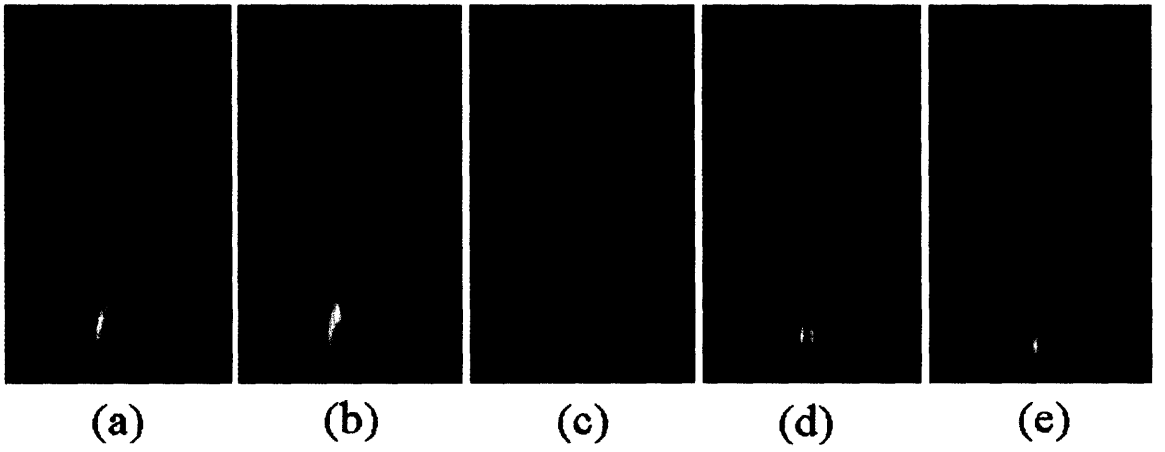

Figure 7: Wingtip views for increasing pitch amplitude, St=0.35 φ=90°;
a) θ_0=0°, b) θ_0=5°, c) θ_0=10°, d) θ_0=15°, e) θ_0=20°

3.4 Phase Angle Effects

From the end view in Figure 8, changing the phase angle between heave and pitch shows minimal changes in the observed wake patterns. Further investigation is warranted to determine whether phase angle significantly affects shedding patterns.

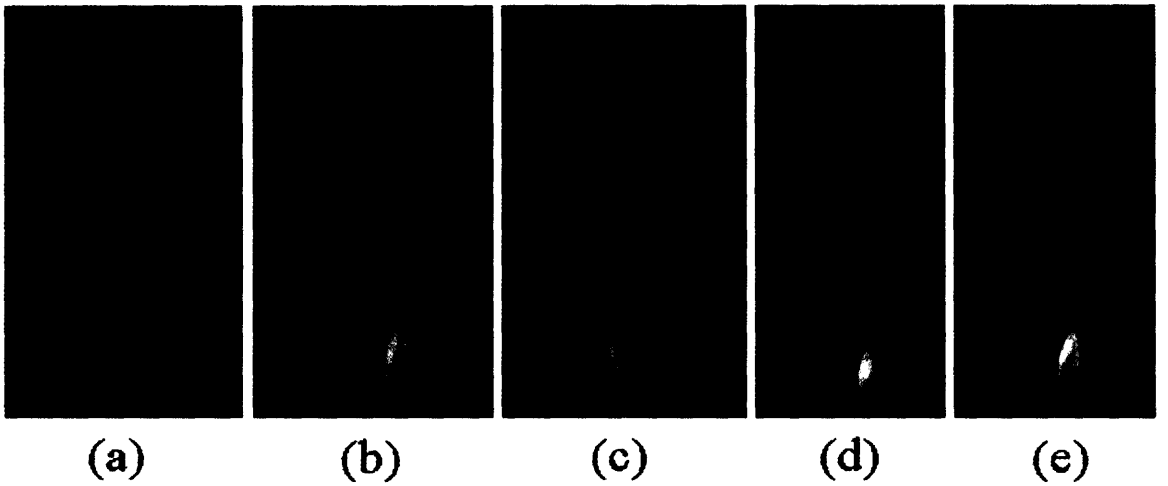

Figure 8: Wingtip views for increasing phase shift, St=0.35 θ_0=10°;
a) φ=60°, b) φ=75°, c) φ=90°, d) φ=105°, e) φ=120°

3.5 Comparison with Previous Works

Figure 9 shows results from Guglielmini, von Ellenrieder et al., and our results; all for the same parameters: St=0.35 θ_0=5° φ=90°. Our results match up nicely with those from Guglielmini. The wingtip view becomes slightly distorted on our image after the second vortex; however, the shapes are very similar to Guglielmini. In the wingtip view from von Ellenrieder et al. you can see the curves of the vortices, but they are not nearly as clean as the other two. The curves on von Ellenrieder et al. are not nearly as pronounced and curved, and they also seem to be drifting upward.

Examining the planform pictures, the rings are evident in each case. First, in Guglielmini the ring is only pronounced for one to two cycles before decreasing lengthwise. This decay is seen in our pictures but to a lesser degree. The rings in von Ellenrieder et al. do not appear to breakdown as rapidly. Also, images from von Ellenrieder et al. show streaks running through the middle of the rings that are not seen in either of the other two cases. This could possibly be explained as a result of the dye injection introducing additional momentum into the wake. In the cases being presented in this thesis, the dye is pulled off of the foil due to the shear in the flow and is thus a less disruptive flow visualization technique.

Similar flow structures are seen in each study, and the main difference appears to be convective forces. von Ellenrieder et al. appears to have the distortion as the vortices appear to be stretched out lengthwise. Then with a small amount of convection our results approach those of Guglielmini whose numerical simulation included no convection due to a free stream velocity. The current setup is more similar to a live fish swimming in a still pond and can hopefully be used to further understand fish swimming hydrodynamics.

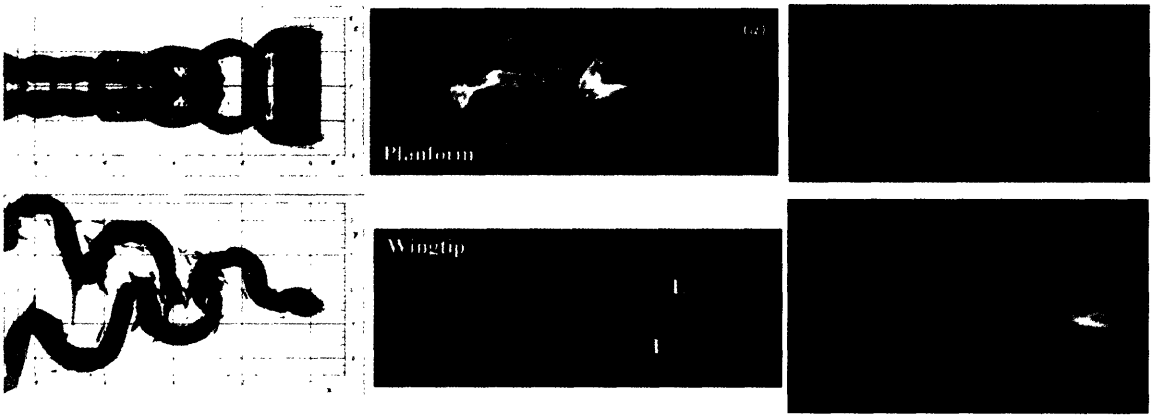

(a) (b) (c)

Figure 9: All pictures for St=0.35 θ_0=5° φ=90°; a) Guglielmini (2004) Fig. 3.12, b) von Ellenrieder et al. (2003) Fig. 3a, c) Our images

Appendix A

Basic Case

St=0.35 θ_0=10° φ=90°

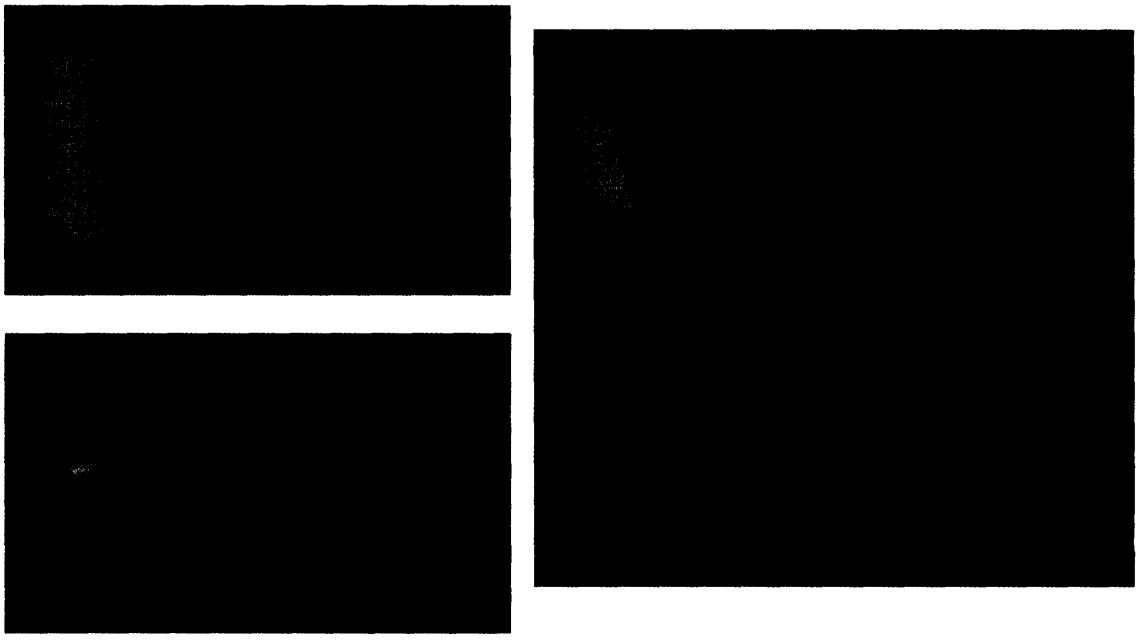

Varying Strouhal Number

St=0.2 θ_0=10° φ=90°

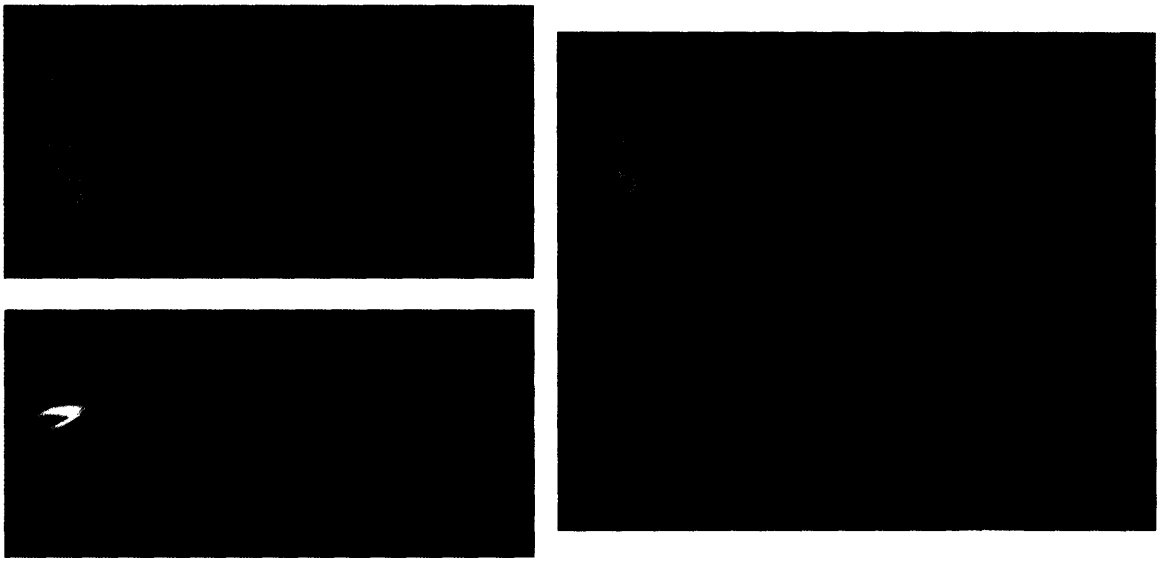

St=0.25 θ_0=10° φ=90°

St=0.3 θ_0=10° φ=90°

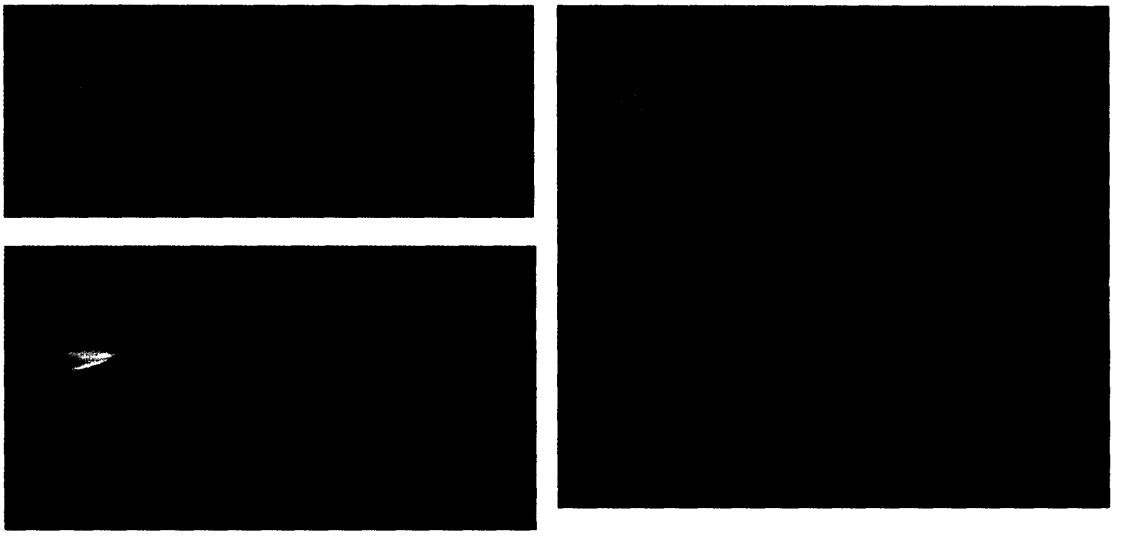

St=0.4 θ_0=10° φ=90°

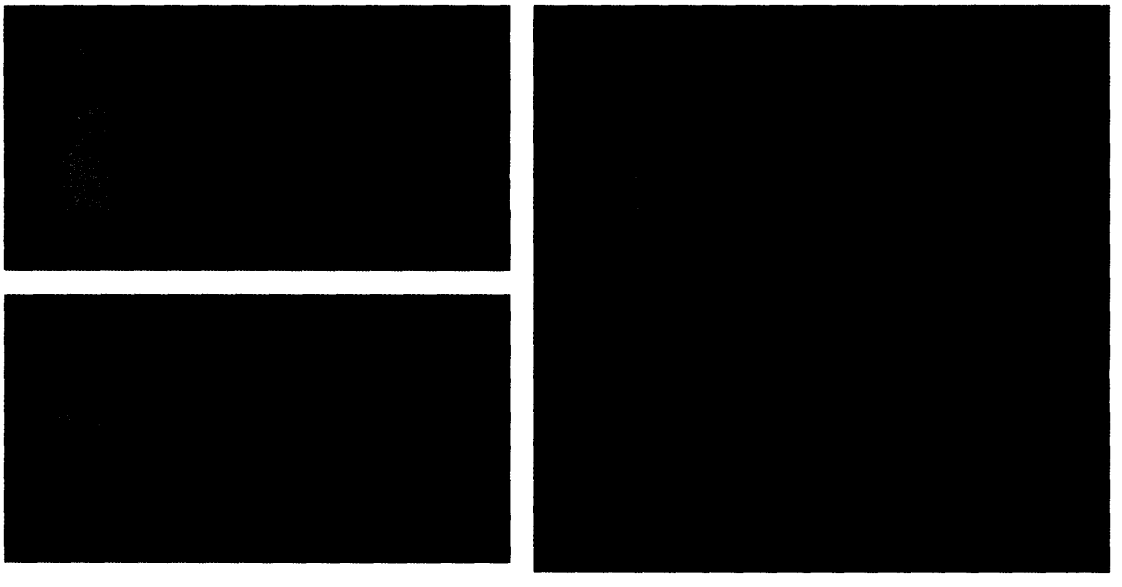

Varying Pitch Amplitude

St=0.35 θ_0=0° φ=90°

St=0.35 θ_0=5° φ=90°

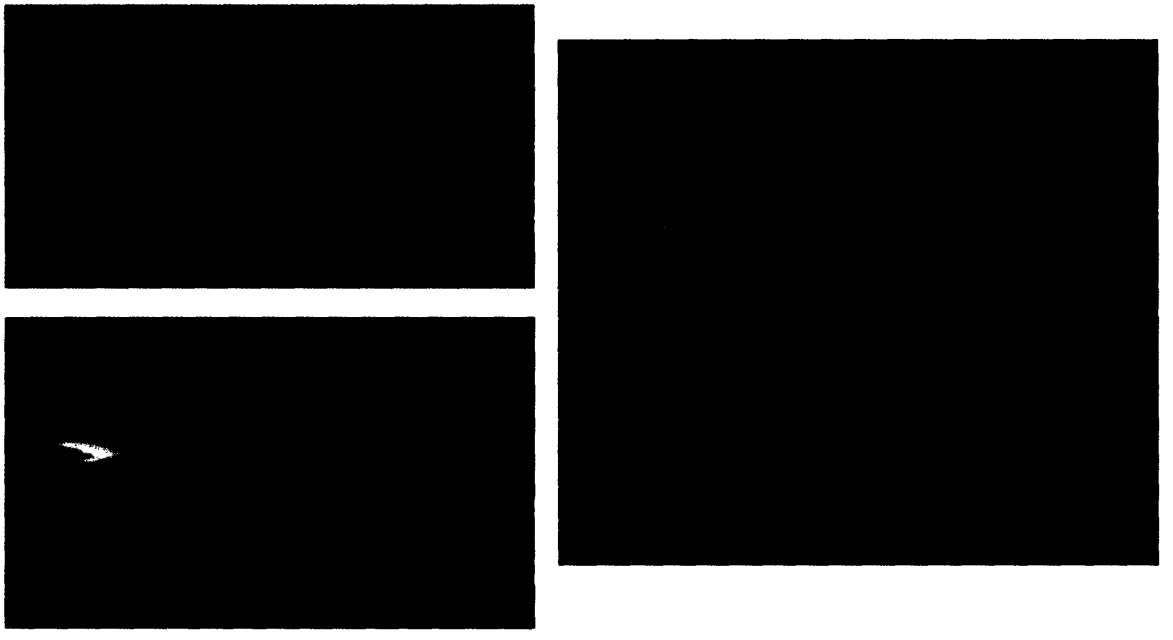

St=0.35 θ_0=15° φ=90°

St=0.35 θ_0=20° φ=90°

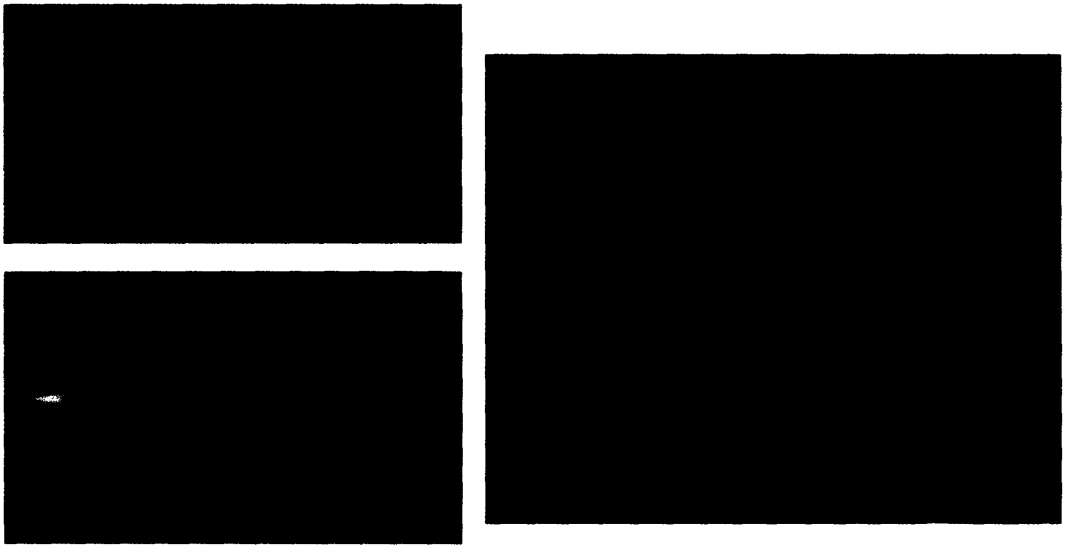

Varying Phase Angle

St=0.35 θ_0=10° φ=60°

St=0.35 θ_0=10° φ=75°

St=0.35 θ_0=10° φ=105°

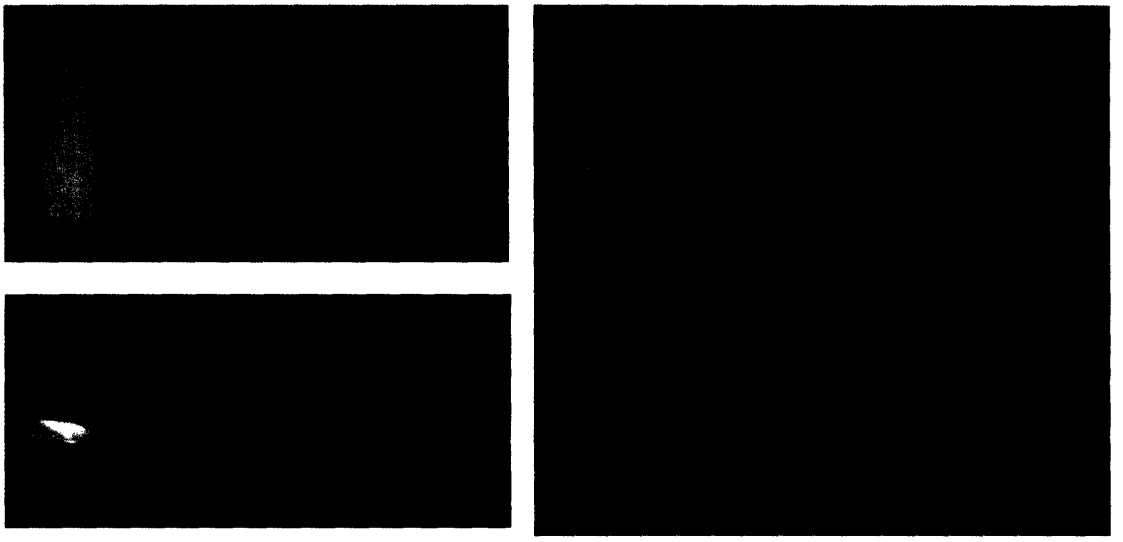

St=0.35 θ_0=10° φ=120°

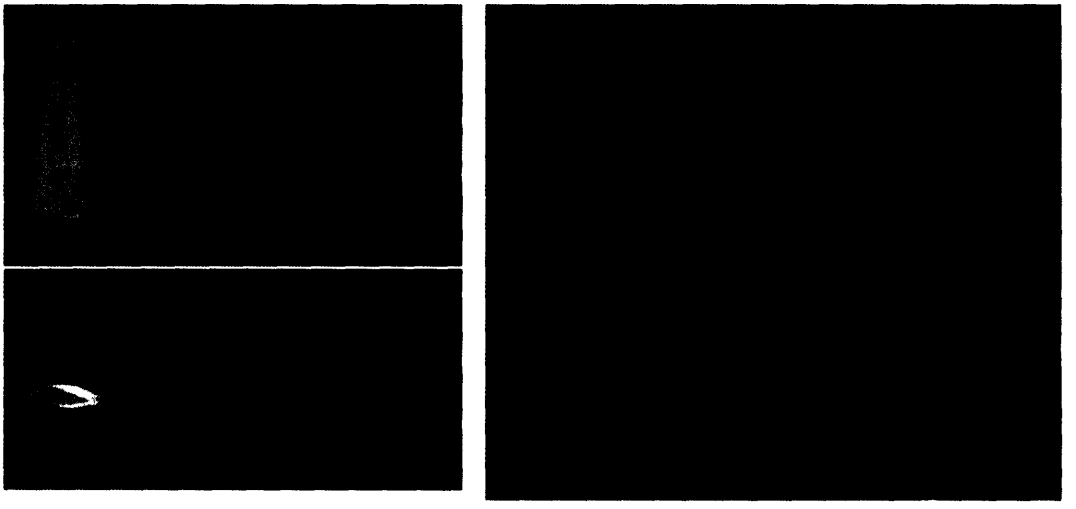

References

[1] Anderson, J.M. Vorticity control for efficient propulsion. PhD thesis, Massachusetts Institute of Technology and Woods Hole Oceanographic Institution, 1996.

[2] Freymuth, P. Propulsive vortical signature of plunging and pitching airfoils. *AIAA Journal*, 26(7):881–883, 1988.

[3] Freymuth, P. Visualizing the connectivity of vortex systems for pitching wings. *Journal of Fluids Engineering*, 111:217-220, 1989.

[4] Guglielmini, L. Modeling of thrust generating foils. PhD thesis, University of Genoa, Department of Environmental Engineering, 2004.

[5] von Ellenrieder, K.D., K. Parker, and J. Soria. Flow structures behind a heaving and pitching finite-span wing. *Journal of Fluid Mechanics*, 490: 129-138, 2003.

MIT Libraries
Document Services

Room 14-0551
77 Massachusetts Avenue
Cambridge, MA 02139
Ph: 617.253.5668 Fax: 617.253.1690
Email: docs@mit.edu
http://libraries.mit.edu/docs

DISCLAIMER OF QUALITY

Due to the condition of the original material, there are unavoidable flaws in this reproduction. We have made every effort possible to provide you with the best copy available. If you are dissatisfied with this product and find it unusable, please contact Document Services as soon as possible.

Thank you.

Some pages in the original document contain color pictures or graphics that will not scan or reproduce well.